# Solar Thermophotovoltaic Converters Based on Tungsten Emitters

**V. M. Andreev**
e-mail: vmandreev@mail.ioffe.ru

**A. S. Vlasov**

**V. P. Khvostikov**

**O. A. Khvostikova**

**P. Y. Gazaryan**

**S. V. Sorokina**

**N. A. Sadchikov**

A.F. Ioffe Physical-Technical Institute RAS,
26 Polytechnicheskaya,
194021 St. Petersburg,
Russia

*Results of a solar thermophotovoltaic (STPV) system study are reported. Modeling of the STPV module performance and the analysis of various parameters influencing the system are presented. The ways for the STPV system efficiency to increase and their magnitude are considered such as: improvement of the emitter radiation selectivity and application of selective filters for better matching the emitter radiation spectrum and cell photoresponse; application of the cells with a back side reflector for recycling the sub-band gap photons; and development of low-band gap tandem TPV cells for better utilization of the radiation spectrum. Sunlight concentrator and STPV modules were designed, fabricated, and tested under indoor and outdoor conditions. A cost-effective sunlight concentrator with Fresnel lens was developed as a primary concentrator and a secondary quartz meniscus lens ensured the high concentration ratio of* $\sim 4000\times$*, which is necessary for achieving the high efficiency of the concentrator–emitter system owing to trap escaping radiation. Several types of STPV modules have been developed and tested under concentrated sunlight. Photocurrent density of* 4.5 $A/cm^2$ *was registered in a photoreceiver based on* $1\times 1$ $cm^2$ GaSb *cells under a solar powered tungsten emitter.*
[DOI: 10.1115/1.2734576]

## 1 Introdution

In a solar thermophotovoltaic (STPV) system, the solar radiation is absorbed and reemitted as thermal radiation before illumination of photovoltaic (PV) cells. Conventional solar PV systems are strongly determined by the sunlight spectrum and by the fact that there is no back connection between a PV cell and the Sun. In STPV systems, the optimization may imply a choice of the emitter spectrum and the possibility to return the unused part of radiation from the receiver back to the emitter surface supplying it by an "additional" power. A STPV system allows us to utilize selective filters/mirrors and sub-band gap photon reflection to the emitter, which results in the efficiency increase. As photons emitted by the TPV cells due to radiative recombination are utilized, the emitter also absorbs these photons using their energy. Owing to this effect, TPV cells would operate in conditions where the generated voltage is higher than in the case of solar PV, when there is no trapping of the emitted photons due to radiative recombination. In solar-powered TPV systems, a high-temperature ($\sim$2000 K) emitter can be used with a good enough "quality" of radiation. As in concentrator photovoltaics, the thermophotovoltaic conversion of the concentrated sunlight is promising for a decrease in cost of solar electricity in comparison with nonconcentrated photovoltaics owing to the reduction of the PV cell area in proportion to an increase of the output electrical power density from the PV cells in high-concentrator STPV systems. The hybrid system with PV conversion (or lighting) for the visible part of sunlight and with TPV conversion for the infrared part of the solar spectrum can be also created ensuring the increase of total efficiency. A possible hybrid solar/fuel thermophotovoltaic unit has an additional advantage: the fuel-fired part of the hybrid system would permit operation at night.

The following key problems arise at optimization of STPV systems: providing high sunlight concentration; tailoring the emission spectrum of the photon emitter; filtering the radiation to utilize photon recycling process and to reduce the thermal impact on the photocells; and tandem cell design allowing increase of PV conversion efficiency of the emitter radiation. These problems may be interconnected. For instance, a selective filter may be deposited directly on the photocell surface reflecting long-wavelength radiation back to the emitter. The role of such a filter may be played by a photocell itself, if there is a mirror on its back surface, which reflects the sub-band gap photons nonabsorbed in the PV cell material.

## 2 Evaluation of the STPV System Efficiency

Theoretical [1–7] and experimental [8–14] studies show an opportunity to achieve a high efficiency in STPV systems. For ideal system elements, maximal theoretical efficiency was found to be 85.4%, which is close to 86.8% of the efficiency of an unlimited stack of tandem cells. Development of STPV converters requires an optimization of system parameters for the best possible performance. In connection with this, an estimation of the maximum achievable efficiency for the STPV converters is of interest. Presented below are the results of calculations of the STPV module efficiency. A schematic drawing of the system considered is shown in Fig. 1. It is assumed that the sunlight is concentrated by means of a focusing system (1) with a concentration ratio (CR) and efficiency ($\eta_C$) in the emitter (2) with the input aperture size providing 90% of the whole concentrated sunlight to hit the aperture. The CR is thus a geometrical parameter, defined as the lens or mirror to the emitter aperture square ratio. The sun's direct radiation was taken as 850 $W/m^2$. The emitter has the shape of a cylinder with a sealed bottom side and is made of tungsten with the emission efficiency $\epsilon(\lambda, T)$ [15]. Thermal radiation of the emitter comes to the photocells (3) with the band gap $E_g$. The emitter temperature is assumed constant over the surface. The unused sub-band gap photons are reflected back to the emitter by the backside mirror (4) or nonabsorbing selective filter with the return efficiency (RE).

The whole system efficiency consists of the following basic components:

- Sunlight concentration and absorption efficiency;
- Thermal radiation efficiency (the emitter efficiency); and

Contributed by the Solar Energy Division of ASME for publication in the JOURNAL OF SOLAR ENERGY ENGINEERING. Manuscript received December 5, 2005; final manuscript received May 10, 2006. Review conducted by Antonio Marti Vega.

  

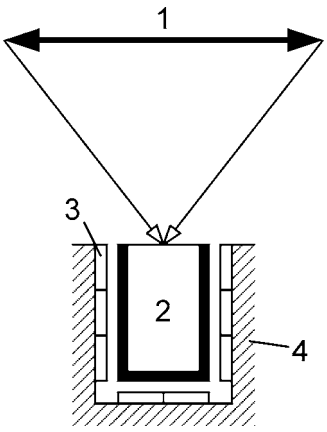


**Fig. 1 Schematic drawing of a STPV system. Major parts shown: (1) solar concentrator: (2) high-temperature emitter; and (3) PV cells; (4) and backside mirror.**

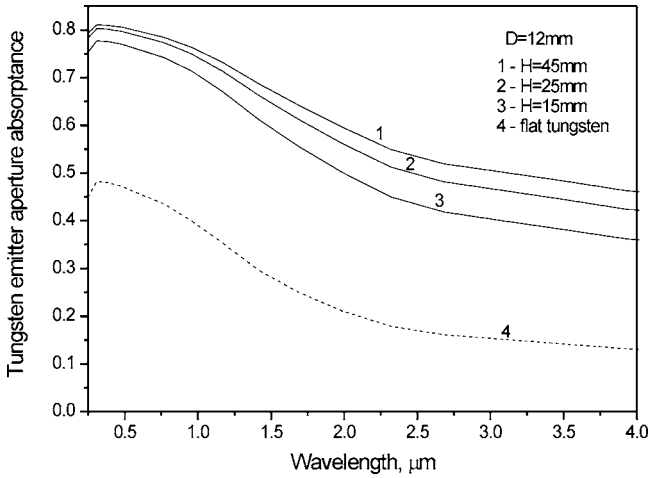


**Fig. 2 Dependence of calculated spectral tungsten emitter aperture absorptansces with diameter of 12 mm and variable emitter length of 15–45 mm. Emitter temperature is *T*=1600 K.**

- Photovoltaic conversion efficiency.

The first parameter appears to be simplest for analysis, because it is clear that the more energy is concentrated on the emitter—the better, and the only aspect that has to be taken into account is the cost of the whole system. At the same time, the absorption of the emitter aperture (AA) should be possibly effective for utilization of the maximum incoming energy. The aperture size should be minimal in order to reduce the part of the thermal radiation emitted through the aperture. As we have shown previously [16], optimization of each parameter (AA, CR, and $\eta_C$) leads to the whole system efficiency increase by several percent. In the STPV system described in this paper concentration ratios of $3.5–5\times10^3\times$ are obtained. Therefore, the calculations are performed for the $8\times10^3$ concentration ratio to account for the future system improvements, and the efficiency of the concentrating system $\eta_C$ was assumed to be 80%, which includes the scattering and absorption losses in the lenses.

Absorption efficiency of a cylinder shaped emitter with a sealed bottom can be calculated according to the theory of cavity thermal emission [17–20] by solving the following set of equations

$$\epsilon_{\text{ef}}(M_i) = \epsilon(M_i) + R(M_i)\left[\int_{F_1} K(M_i,N_1)\epsilon_{\text{ef}}(N_1)dF_{N_1} + \int_{F_2} K(M_i,N_2)\epsilon_{\text{ef}}(N_2)dF_{N_2}\right] \quad (1)$$

where $\epsilon_{\text{ef}}(N)$=the effictive emissivity of the aperture; $K(M_i,N)$=geometrical coefficient describing view angle of heat exchanging surfaces (the view angle of an elementary square on one surface to an elementary square on another surface); $F_1$, $F_2$=cylindrical and flat surfaces of the emitter; $\epsilon(M_i)$=emissivity; and $R(M_i)$=reflectance of cavity material. Precise calculation implies multiple order of reflection to ensure equality of the heat emitted by the cavity surface and the heat absorbed by the cavity itself and emitted through the aperture. Figure 2 presents the results of such calculation for tungsten emitters with 12 mm diameter and 15–45 mm lengths. Absorption efficiency of cylindrical tungsten emitters appears to be about 0.6–0.7 for the AM1.5 solar spectrum. This parameter can be increased by a combination of different materials, such as use of polycrystalline SiC or pyrographite inside the aperture.

The emitter temperature was calculated by solving the energy flux Eq. (2), i.e., the incoming energy should be equal to the outcoming in a steady state

$$E_{\text{inc}} + E_{\text{return}} = E_{\text{rad}} + E_{\text{conv}} \quad (2)$$

Here $E_{\text{inc}}$=solar energy, absorbed by the emitter; $E_{\text{return}}$=the part of unused sub-band gap radiation returned to the emitter; $E_{\text{conv}}$=convectional losses; and $E_{\text{rad}}$=energy, irradiated by the emitter, defined by Stefan–Boltzmann law as $\mu\sigma T^4$. The efficiency of emitter radiation (emitter efficiency) is determined as the ratio of the energy part illuminating the PV cells to the total energy irradiated by the emitter (including that through the input aperture). In the ideal case, when all available space is covered with PV cells, the emitter efficiency is described as a geometrical parameter, determined by the emitter length and its diameter. The longer the emitter, the higher its efficiency, but the lower the achievable temperature. In Fig. 3 (left scale) the emitter efficiency is shown versus the emitter temperature for two concentration ratios of 2000× and 8000×.

The PV conversion efficiency (Fig. 3, right scale) was calculated assuming the following conditions: a Shockley–Queisser model was used, i.e., all photons above the band gap are absorbed, producing photocurrent and the only recombination process available is radiative recombination. This implies the current–voltage equation

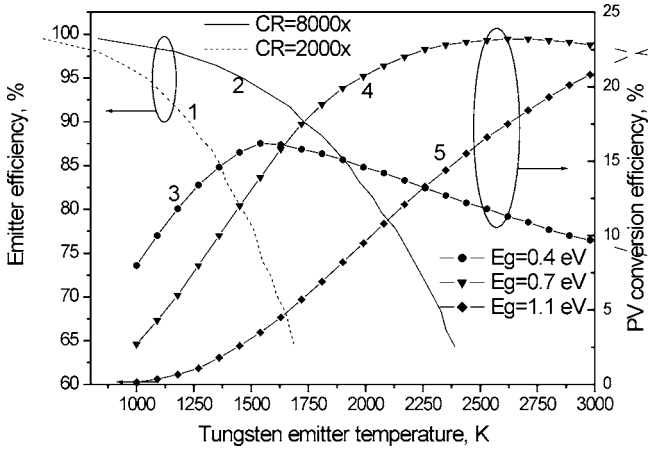


**Fig. 3 Dependence of calculated emitter efficiency for two concentration ratios (CR)=2000x and 8000x (left) and PV conversion efficiency for three band gaps of 0.4 eV, 0.7 eV, and 1.1 eV (right) from tungsten emitter temperature**

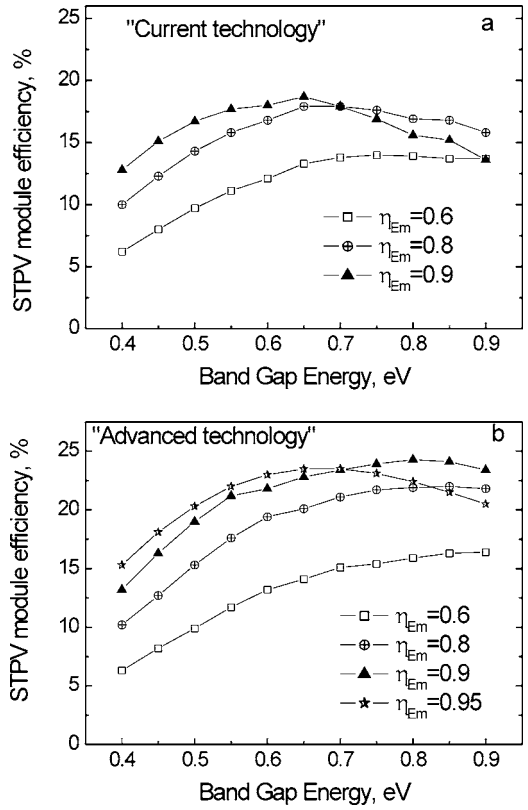


**Fig. 4 Dependence of calculated efficiency of STPV module versus single-junction PV cell band gap for different values of tungsten emitter efficiency the $\eta_{Em}$ and two system configurations: (*a*) current technology (AA=0.7, RE=0.5); and (*b*) advanced technology (AA=0.9; RE=0.9)**

$$I = I_0 \exp\left(\frac{eU}{k_B T}\right) \tag{3}$$

where $I_0$ is the PV cell radiative current density, which depends on the PV cell meterial properties and is given by Eq. (4) [21]

$$I_0 = \frac{e(n^2+1)E_g^2 k_B T}{4\pi^2 \hbar^3 c^2} \exp\left(-\frac{E_g}{k_B T}\right) \tag{4}$$

No ohmic losses are considered. But in order to avoid nonachievable extremely high current values, the current density was limited to 5 A/cm$^2$, increasing the number of PV cells where needed. Photons with the energy below the band gap are reflected back to the emitter with the efficiency RE by means of a backside mirror or selective filter and are absorbed in the emitter with the corresponding absorption efficiency. The rest of radiation is reflected back again to the PV cells and so on. This process can be described as reducing geometric series.

In Fig. 3 (right scale) the PV conversion efficiency is shown for three different band gaps versus emitter temperature. It is clear from the figure that analysis of the system efficiency must be complex, including all the influencing terms, because variation of different parameters (CR, $\eta_{Em}$, $E_g$, etc.) leads to a different system configuration: increasing emitter efficiency is accompanied by the temperature decrease which can reduce PV conversion efficiency and vice versa, higher concentration ratio shifts the emitter efficiency to higher temperature values, which are optimal for wider band gap material, etc.

While constructing the system there are two important interconnected factorors that need to be chosen: PV cell band gap and efficiency of emitter. Figure 4 presents the STPV module efficiency dependence on the band gap of a single junction PV cell

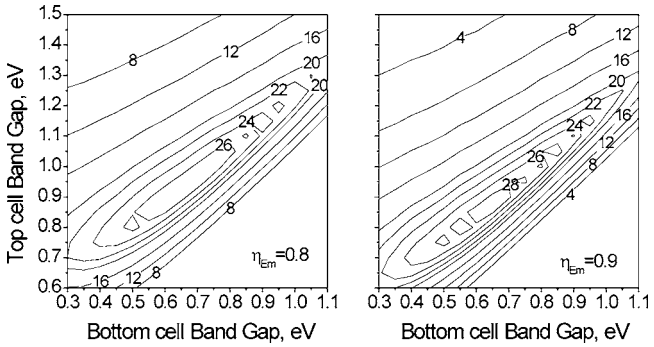


**Fig. 5 Calculated efficiency of STPV module (advanced technology) with the use of monolithic tandem PV cells for various tungsten emitter efficiencies $\eta_{Em}$. The graphs are plotted for various top and bottom band gaps as a set of isoefficiency lines.**

for different values of the emitter efficiency. Two principal system configurations are considered: "current technology"—with parameters AA=0.7 and RE=0.5 close to those available (Fig. 4(*a*)) and "advanced technology" (Fig. 4(*b*)) with AA=0.9 and RE=0.9. Optimization of these parameters is the subject of further development. As can be seen from Fig. 4, optimization of the sunlight absorption and unused light recirculation processes leads to a sufficient increase in the STPV module efficiency accompanied by an increase in the optimal band gap and emitter efficiency. This originates partly due to the increase in emitter temperature of the fixed efficiency by 300–400 deg. It is interesting to notice that independently of the system configuration, the maximum STPV efficiency is obtained with the emitter temperature in the range of 1800–2300 K. Thus, according to the calculations presented, the maximum STPV efficiency of our GaSb based STPV module with a tungsten emitter may reach 18% for current technology with possible improvement to 25%.

In modern photovoltaics, monolithic tandem PV cells are widely used for PV conversion efficiency increase [22]. Below we present an analysis of STPV performance with the use of monolithic tandem PV cells in order to estimate the possible benefits of the multijunction cells in a STPV system. Figure 5 shows a set of graphs with calculated isoefficiency curves, plotted against top and bottom cell band gaps. The graphs are calculated for different emitter efficiencies in the "advanced technology" case. Comparing these data with that of the single junction (Fig. 4(*b*)) it can be seen that efficiency increases by 4–5%. However, it should be noted that since the monolithic tandem PV cells should always be adjusted with the incoming spectrum to implement an equal current requirement, the change of the sunlight intensity during daily operation may lead to a significant emitter temperature change, accompanied by the emission spectrum blue/red shift. In Fig. 6 the calculated STPV efficiency is plotted against the bottom cell band gap (assuming the top cell is always optimal) for three different sunlight intensities: 600 W/cm$^2$, 800 W/cm$^2$, and 1000 W/cm$^2$. Calculations are presented for the "current technology" case. One can see a shift of the maximum toward lower band gap values with incoming energy decrease. However this effect is not critical and an average point may be chosen with only 1–2% efficiency loss retaining 22–23% of the total efficiency for the "current technology" case and 26–27% for the "advanced technology."

Another way to improve the PV conversion efficiency is in the increase of emitter radiation selectivity, so that the emitter radiation is matched to the band gap of the photoreceiver. It may be depositing the rare earth oxides on the irradiating emitter surface, use of textured tungsten (photonic crystal), etc. [23–25].

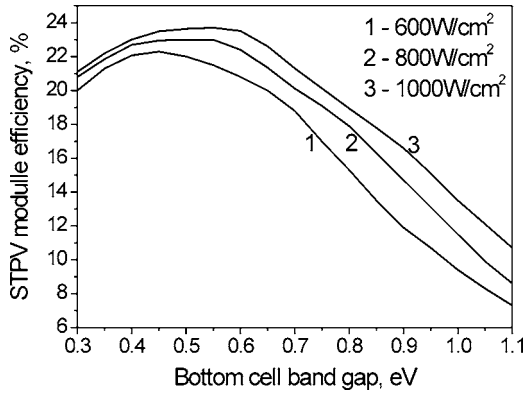


**Fig. 6 Calculated efficiency of STPV module (current technology) with tandem PV cells for different direct sun radiation levels and emitter efficiency of 0.8. The graph is plotted versus bottom cell band gap with the optimal top cell band gap.**

## 3 Design and Performances of Sunlight Concentrators for STPV Systems

An ideal solar concentrator is a parabolic mirror with an opening angle of 180 deg. It may allow the maximum achievable concentration ratio of more than 40,000×. Such a mirror, however, is very difficult to fabricate. Also, the cost of quality mirrors is high. Systems with the lower opening angle demonstrate accordingly lower concentration ratios. The most cost-effective concentrating system is obtained by the use of a large square Fresnel lens. The concentration ratio is determined basically by the diameter to focal length ratio and is limited by the angle of incidence of the sunlight to the lens surface. Normally the lens diameter should be lower than the focal length for maximum Fresnel lens efficiency. This gives the concentration ratios of $1–2\times10^3\times$ and corresponds to an opening angle of 50–70 deg. The concentration ratio may be increased by introducing a secondary element such as a focon (CPC) or a quartz lens. In a focon, however, a retracing of incoming rays takes place, and at the output the light tends to have a 180 deg opening angle. This requires that the emitter should be placed closely to the focon, which is difficult, considering high emitter temperatures. Inserting a quartz lens as a secondary element increases the opening angle of incoming light, thus reducing the spot size. This may increase the concentration ratio by several times. Use of a specially prepared convex–concave quartz lens ensures minimal scattering losses.

Figure 7 presents a two-stage sunlight concentrator system. It consists of a Fresnel lens (0.36 $m^2$ in area and 0.75 m focal length) and a secondary quartz meniscus lens. 90% of concentrated sunlight is collected in the spot of 10 mm diameter. The light distribution inside the spot was measured by scanning with a GaSb PV cell with a 1-mm-diameter aperture mounted on a water cooled stage. A concentration ratio of 3600× is ensured by this construction, the main advantage of which is its low cost. However, the material (PMMA) of the Fresnel lens is characterized by poor outdoor stability. Recently, a new technology for Fresnel lenses of composite structure was developed at the Ioffe Institute [26]: the microprisms are formed from transparent silicone rubber contacting with the front silicate glass sheet as a protective superstrate. The formation process developed allows fabricating the lens of total area of 0.6 m × 0.6 m. This type of Fresnel lens ensures much better environmental stability owing to the use of high stable silicate glass, protecting the Fresnel lens made of silicone rubber, which is also characterized by a high stability under the action of outdoor conditions. These Fresnel lenses are very promising for fabrication of concentrator PV modules [26] and have perspectives for use in low-cost STPV systems.

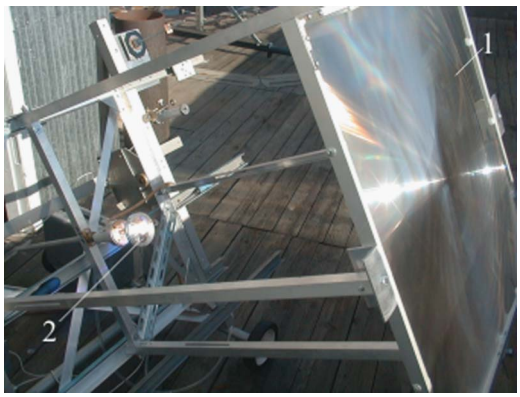


**Fig. 7 Two-stage concentrator based on a Fresnel lens (1) and a quartz meniscus lens (2)**

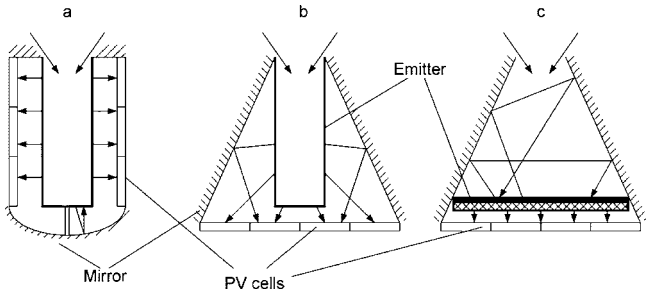


**Fig. 8 Schematic drawings of the developed cylindrical (*a*) and conical (*b*), (*c*) STPV modules**

## Solar TPV Module Designs

Basic demands for an emitter are: it should absorb a maximum of incoming sunlight and produce a selective emission to PV cells. The simplest way to satisfy these conditions is to make a sealed bottom cylinder shaped emitter of tungsten with a partly selective emission spectrum. In this case two types of TPV systems are available: cylindrical (Fig. 8(*a*)) and conical (Figs. 8(*b*) and 8(*c*)). The emitter is placed in a quartz chamber filled with a rare gas (Ar or Xe) to prevent it from oxidation. In the conical system (Figs. 9(*a*) and 9(*b*)) the thermal radiation is reflected to PV cells by an Au coated cone-shaped mirror, and PV cells are mounted on a flat basement. In the cylindrical system the PV cells surround the emitter, which are mounted on the inner side of a cooled cylindrical base(Fig. 9(*c*)). Both modules were tested outdoors under the direct sun illumination. The direct sun irradiation was measured to be 800–850 $W/m^2$ (summer and autumn 2005, St.Petersburg, Russia). Emitter temperature was registered by both a pyrometer and a W–Re thermocouple. In Fig. 10(*a*) a 45 mm long tantalum emitter is shown installed in the cylindrical setup and heated by a Fresnel lens. Temperatures in the range of 1400–1900 K were obtained, depending on the emitter size and material. Figure 11 a shows a dependence of tantalum emitter temperature for different

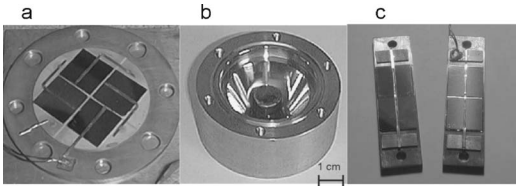


**Fig. 9 STPV module with a flat PV receiver (*a*), a tungsten emitter surrounded by a conical reflector (*b*), and a complete module (*c*)**

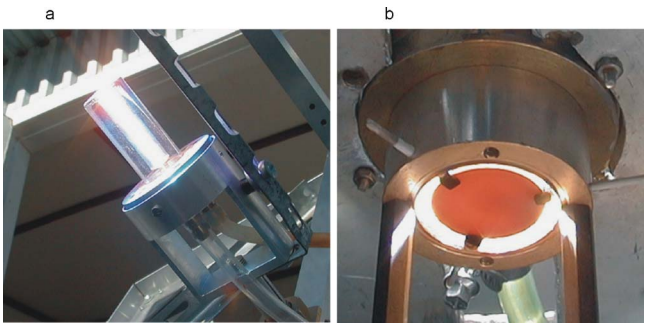


**Fig. 10** (*a*) **Tantalum emitter (12 mm in diameter and 45 mm length), installed in the STPV modulle of "cylindrical" type and heated by Fresnel lens; and (*b*) SiC flat emitter installed in the conical system and heated with the solar simulator system (~200 W at the input of the aperture) [28]**

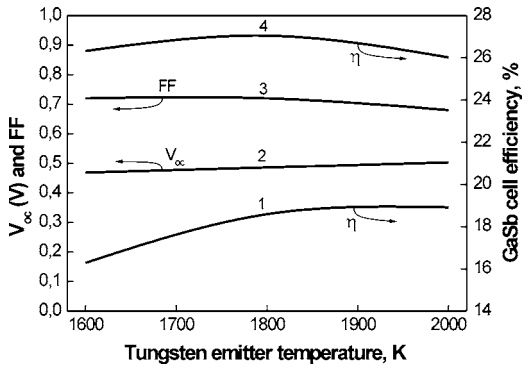


**Fig. 12 Open circuit voltage ($V_{OC}$, curve 2), fill factor (FF), (curve 3), and efficiency (curves 1,4) of GaSb TPV cell as a function of tungsten emitter temperature. Efficiency was estimated under the following radiation conditions: under the full radiation spectra (curve 1) and under spectra cutoff at λ >1820 nm (curve 4)**

emitter sizes [27]. All emitters presented were made with the same aperture of 12 mm (95% of concentrated energy is collected) and varied with the cylinder length. The emitter temperature was recalibrated to ensure equal direct sun intensity of 800 W/m$^2$ for better comparison. It is seen that the emitter temperature grows with the decreasing emitter size. Theoretical calculation of the emitter temperature is shown in Fig. 11(*a*) with a dotted line. It can be seen that longer emitters show temperature even lower than expected. This is explained by growing convectional losses that accompany the increasing emitter surface, which was not taken into account.

In the conical system the number of PV cells is fixed by its construction (~5 cm$^2$ in the Fig. 9 module), and the dependence of the radiation density on the emitter temperature is indirect. In fact, the energy irradiated by the emitter is always the same, and changing its efficiency will change the part of radiation that goes back to the air on one hand, but on the other hand it will shift the emission spectrum. This process needs special consideration.

Another "flat" type of the emitter may be realized in the conical system (Figs. 8(*c*) and 10(*b*)). The advantage of such a configuration is a flat emitter surface, which is good for the selectivity enhancement (such as photolithography, oxide deposition, etc.). However, the input emitter surface must be blackened and a high-quality cone mirror has to be used to ensure efficient sunlight absorption in the emitter. Figure 10(*b*) shows a SiC plate mounted in the conical system and heated by the Sun Simulator system [28].

GaSb TPV cells were fabricated with the use of Zn diffusion and liquid-phase epitasy (LPE) technologies. In the first experiments the cells were mounted in parallel on a copper heat sink. To ensure the series connection of the cells, the heatsink substrate with high thermal conductivity must be an electrical insulator [29,30]. For fabrication of photoreceivers, we have selected BeO ceramics, which has the electrical resistivity of more than $10^{14}$ Ω/cm with the best thermal conductivity of 250 W/K m. The thermal expansion coefficient of BeO ceramics is $6 \cdot 10^{-6}$ K$^{-1}$ being close to that of GaSb in the temperature range of 20–150 °C. Contact composition Mo/Ni/Au to the BeO substrate allowed us to solve the problem of adhesion of GaSb cells to ceramics. The cell efficiency of 19% under illumination by a tungsten emitter heated up to 1900–2000 K had been derived from experimentally measured PV parameters (Fig. 12). This value is close to the theoretical maximum of ~22%(see Fig. 2) for GaSb cells illuminated by tungsten. Cell efficiency as high as 27% was estimated for the spectrum cutoff at λ > 1820 nm (conditions of 100% return efficiency for sub-band gap photons). In the conical module the photocurrent density $J_{SC}$=4.5 A/cm$^2$, open circuit voltage $V_{OC}$=0.49 V, and fill factor (FF)=0.68 have been measured in a GaSb cell under the solar powered emitter heated to the temperature of about 2000 K.

Figure 13 shows the average thermal irradiation density (in cylindrical system), measured with a GaSb cell (curve 1, left scale). The average short circuit current grows with increasing emitter temperature (smaller emitter length). However the total estimated power output of the system (curve 2 in Fig. 13, right scale) has a maximum for emitters of 35–45 mm in length. This corresponds

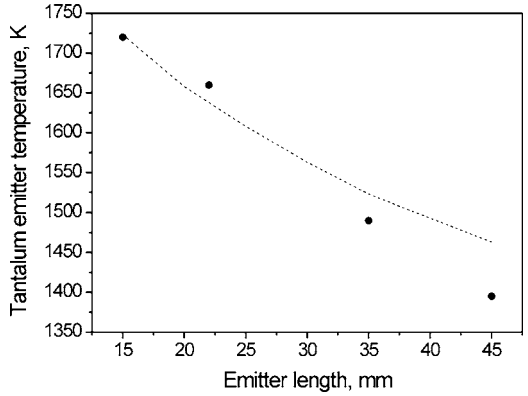


**Fig. 11 (Circles) measured tungsten emitter temperature as a function of emitter length (emitter diameter is 12 mm and direct sun irradiation density is normalized to 800 W/m$^2$); and (dotted line) calculated emitter temperature**

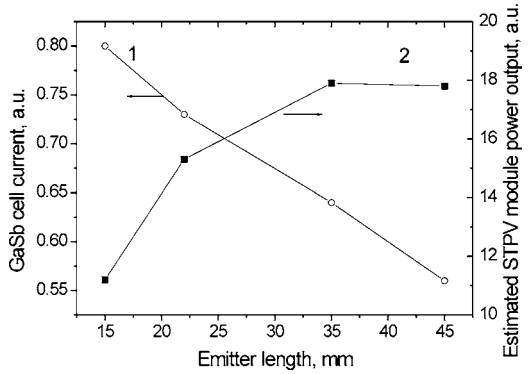


**Fig. 13 Average measured thermal irradiation density (GaSb cell short circuit current) (curve 1), left scale, and the estimated STPV module power output (curve 2), right scale plotted for different emitter lengths**

to the emitter efficiencies of 0.8–0.85, as expected in the above calculations (see Fig. 3(*a*)). The emitter temperatures are, however, lower than expected. This is explained by several factors affecting the system performance: no return of unused radiation is yet realized in the system and also convectional and unforced radiational losses should be minimized in order to achieve the expected module efficiency.

## 4 Conclusion

Research and development of a solar TPV system have been presented. The solar concentrator developed, based on a Fresnel lens, does not show the maximum performance possible (a parabolic mirror would give higher concentration ratios and efficiency), however it has the great advantage of low price, still allowing us to reach high concentrations up to 4000x. The conical module developed allows the use of flat emitters, which is preferable for the pilot studies of new materials application. At the same time, a cylindrical system is preferable for the final system production for several advantages: it may consist of several stacked modules, the cooling of PV cells is easier, and it is more suitable for the use in hybrid solar/fuel fired systems, which are promising for totally self-contained units. The GaSb PV cells developed are most relevant for the use in such systems. As it is shown by our calculations, maximum achievable efficiency for a module with a tungsten selective emitter is 23–25% with the band gap energy of single-junction photovoltaic cells $E_g$=0.7–0.9 eV. The use of monolithic tandem cells is questionable, as an expected increase in total efficiensy is only 2–3% percent, which may also be neglected by the losses in tunnel junction, for example. BeO ceramics is preferable for the cascade sell assembly. System performance is examined with a cylindrical shaped tantalum emitter and ways of possible improvement (convectional and radiation losses decrease, aperture blackness etc.) are proposed.

## Acknowledgment

The authors would like to thank Zh. Alferov, A. Luque, C. Algora, C. Jaussaud, A. Bett, A. Gombert, W. Durish, and W. Tobler for support and fruitful discussions. The authors thank V. Grilikhes, O. Chosta, and N. Davidiuk for the contribution to this work. This work has been supported by the European Commission through the funding of the project FULLSPECTRUM (Contract SES6-CT-2003-502620).

## References

[1] Spirkl, W., and Ries, H., 1985, "Solar Thermophotovoltaics: An Assessment," J. Appl. Phys., **57**(9), pp. 4409–4414.
[2] Davies, P. A., and Luque, A., 1994, "Solar Thermophotovoltaics: Brief Review and a New Look," Sol. Energy Mater. Sol. Cells, **33**, pp. 11–22.
[3] Luque, A., and Marti, A., 1999, "Limiting Efficiency of Coupled Thermal and Photovoltaic Converters," Sol. Energy Mater. Sol. Cells, **58**, pp. 147–165.
[4] Badescu, V., 2001, "Thermodynamic Theory of Thermophotovoltaic Solar Energy Conversion," J. Appl. Phys., **90**(12), pp. 6476–6486.
[5] Harder, N.-P., and Würfel, P., 2003, "Theoretical Limits of Thermophotovoltaic Solar Energy Conversion," Semicond. Sci. Technol., **18**, pp. S151–157.
[6] Cody, G. D., 1998, "Theoretical Maximum Efficiencies for Thermophotovoltaic Devices," *Proceedings 4th NREL Conference on TPV Generation of Electricity*, Vol. 460, Denver, CO, 11–14 October 1998, pp. 58–67.
[7] Andreev, V. M., Khvostikov, V. P., Khvostikova, O. A., Rumyantsev, V. D., Gazarjan, P. Y., and Vlasov, A. S., 2004, "Solar Thermophotovoltaic Converters: Efficiency Potentialities," AIP Conf. Proc., **738**, pp. 96–104.
[8] Stone, K. W., Fatemi, N. S., and Garverick, L., 1996, "Operation and Component Testing of a Solar Thermophotovoltaic Power System," *Proceedings 25th IEEE Photovoltaic Solar Energy Conference*, Washington, D.C., 13–17 May 1996, pp. 1421–1424.
[9] Yugami, H., Sai, H., Nakamuro, K., Nakagama, N., and Ohtsuko, H., 2000, "Solar Thermophotovoltaic Using $Al_2O_3/Er_3Al_5O_{12}$ Eutectic Composite Selective Emitter," *Proceedings 28th IEEE Photovoltaic Solar Energy Conference*, Anchorage, AK, 15–22 September 2000, pp. 1214–1217.
[10] Andreev, V. M., and Khvostikov, V. P., 2003, "Solar Thermophotovoltaic Converters," *Proceedings of 3rd JRC Workshop* The Path to Ultra-high Efficient Photovoltaics, Ispra, Italy, 2–3 October 2003, pp. 83–102.
[11] Rumyantsev, V. D., Khvostikov, V. P., Gazaryan, P. Y., Khvostikova, O. A., Sadchikov, N. A., Vlasov, A. S., Ionova, E. A., and Andreev, V. M., 2004, "Structural Features of Solar TPV Systems," AIP Conf. Proc., **738**, pp. 79–87.
[12] Khvostikov, V. P., Rumyantsev, V. D., Gazaryan, P. Y., Khvostikova, O. A., Kaluzhniy, N. A., and Andreev, V. M., 2004, "TPV Cells Based on Ge, GaSb and InAs Related Compounds for Solar Powered TPV Systems," *Proceedings of the 19th European Photovoltaic Solar Energy Conference*, Paris, France, 7–11 June 2004, pp. 105–108.
[13] Khvostikov, V. P., Rumyantsev, V. D., Shvarts, M. Z., Khvostikova, O. A., Gazaryan, P. Y., Sorokina, S. V., Kaluzhniy, N. A., and Andreev, V. M., 2004, "Thermophotovoltaic Cells Based on Low-Bandgap Compounds," AIP Conf. Proc., **738**, pp. 436–444.
[14] Horne, E., 2002, "Hybrid Thermophotovoltaic Power Systems," http://www.energy.ca.gov/pier/final_project_reports/500-02-048F.html.
[15] Malyshev, V. I., 1979, *Introduction to Experimental Spectroscopy*, Nauka, Moscow, Russia (in Russian).
[16] Andreev, V. M., Khvostikov, V. P., Khvostikova, O. A., Vlasov, A. S., Gazaryan, P. Y., Sadchikov, N. A., and Rumyantsev, V. D., 2005, "Solar Thermophotovoltaic System with High Temperature Tungsten Emitter," *Proc. 31st IEEE Photovoltaic Specialist Conference*, Orlando, FL, 3–7 January 2005, pp. 671–74.
[17] Rusin, S. P., and Peletsky, V. E., 1987, *Thermal Irradiation of Cavities*, Energoatomizdat, Russia, Chap. 5 (in Russian).
[18] Bedford, R. E., Ma, C. K., Chu, Z., Sun, Y., and Chen, S., 1985, "Emissivities of Diffuse Cavities. IV: Isothermal and Nonisothermal Cylindro-Inner-Cones," Appl. Opt., **24**(18), pp. 2971–2980.
[19] Bedford, R. E., and Ma, C. K., 1975, "Emissitivies of Diffuse Cavities, II: Isothermal and Nonisothermal Cylindro-Cones," J. Opt. Soc. Am., **65**(5), pp. 565–572.
[20] Bedford, R. E., and Ma, C. K., 1975, "Emissitivies of Diffuse Cavities, II: Isothermal and Nonisothermal Cones and Cylindres," J. Opt. Soc. Am., **64**(3), pp. 339–349.
[21] Henry, C. H., 1980, "Limiting Efficiencies of Ideal Single and Multiple Energy Gap Terrestrial Solar Cells," J. Appl. Phys., **51**(8), pp. 4494–4500.
[22] Andreev, V. M., 2004, "Solar Cells for TPV Converters," in *Next Generation Photovoltaics. High Efficiency through Full Spectrum Utilization*, IoP, Bristol, U.K., Chap. 11, p. 246.
[23] Gombert, A., 2003, "An Overview of TPV Emitter Technologies," AIP Conf. Proc., **653**, pp. 123–131.
[24] Lin, S. Y., Moreno, J., and Fleming, J. G., 2003, "Three-Dimensional Photonic-Crystal Emitter for Thermal Photovoltaic Power Generation," Appl. Phys. Lett., **83**, pp. 380–382.
[25] Bitnar, B., Durisch, W., Palfinger, G., von Roth, F., Vogt, U., Bronstrup, A., and Seiler, D., 2004, "Practical Thermophotovoltaic Generators," Semiconductors, **38**, pp. 941–945.
[26] Rumyantsev, V. D., Chalov, A. E., Ionova, E. A., Larionov, V. R., and Andreev, V. M., 2004, "Concentrator PV Modules with Multi-Junction Cells and Primary/Secondary Refractive Optical Elements," *Proceedings of the 19th European Photovoltaic Solar Energy Conference*, Paris, France, 7–11 June 2004, pp. 2090–2094.
[27] Tantalum was chosen as the emitter material in preliminary tests for its emissivity is close to tungsten one, but it is better for mechanical treatment.
[28] Andreev, V. M., Khvostikov, V. P., Rumyantsev, V. D., Khvostikova, O. A., Gazaryan, P. Y., Sadchikkov, N. A., Sorokina, S. V., Zadiranov, Y. M., and Shvarts, M. Z., 2005, "Thermophotovoltaic Converters with Solar Powered High Temperature Emitters," *Proc. 20th Europeen Photovoltaic Solar Energy Conference*, Barcelona, Spain, 6–10 June 2005, pp. 8–13.
[29] Doyle, E. F., Becker, F. E., Shukla, K. C., and Fraas, L. M., 1999, "Design of a Thermophotovoltaic Battery Substitute," AIP Conf. Proc., **460**, pp. 351–361.
[30] Schlegl, T., Dimroth, F., Ohm, A., and Bett, A. W., 2004, "TPV Modules Based on GaSb Substrates," AIP Conf. Proc., **738**, pp. 285–293.